

Ink-jet printing of ceramic pillar arrays

X. ZHAO*, J. R. G. EVANS, M. J. EDIRISINGHE
 Department of Materials, Queen Mary, University of London,
 Mile End Road, London E1 4NS, UK

J. H. SONG
 Department of Mechanical Engineering, Brunel University,
 Uxbridge, Middlesex, UB8 3PH, UK

A high performance 500 nozzle in-line piezoelectric drop-on-demand print-head mounted on a linear table with z-axis control was used to prepare arrays of fine ceramic pillars. Such structures may find applications in miniature heat exchangers, catalyst supports, for cell up-regulation in prosthetics or in polymer-ceramic piezoelectric 1-3 composites. The ink conveyed 14 vol% fine zirconia and deposited a wax-based suspension in an octane-alcohol mixture. The dried ink contained 63 vol% zirconia. © 2002 Kluwer Academic Publishers

1. Introduction

Direct ceramic ink-jet printing has emerged as a pathway for solid freeforming ceramics [1, 2] and a range of printers can be used [3–8]. It provides a capability for, *inter alia*, engineering miniature components [9] and making functionally graded materials [10]. Ceramic sols [11] or precursor solutions [12] can be used as inks. It therefore complements other solid freeforming procedures such as stereolithography [13], selective laser sintering [14] or fused deposition modelling [15]. The present work is part of our attempt to explore the strengths and weaknesses of direct ceramic ink-jet printing and to identify the areas where it can make a useful contribution. It is also part of a systematic and extensive exploration of the compatibility of ceramic suspensions with a wide range of ink-jet printer types.

Composites designated 1-3 in Newnham's taxonomy [16] have a wide range of applications. For instance, 1-3 piezoelectric ceramic-polymer composite transducers have applications in medical imaging and non-destructive evaluation [17, 18]. Such arrays could also find application in situations where gas-solid interactions are needed, such as heat exchangers and catalyst supports. Osteoblast cells are known to up-regulate in response to a profiled surface [19].

Arrays of ceramic pillars were first made using a drop-on-demand ink-jet printer [9]. A fine zirconia suspension in alcohol was used as the ink and passed directly through the nozzle. Arrays of lead zirconate titanate (PZT) pillars for 1-3 polymer-ceramic composites have been made by direct ink-jet printing [20]. Partly due to the relatively low ceramic volume fraction (0.5) in the dried ink, deformation occurred during binder removal and sintering. Hollow tubes have been made by a similar method [21].

Previous work carried out in this laboratory has demonstrated the feasibility of using a high speed multi-

nozzle drop-on-demand printer made by Xaar Ltd, Cambridge, UK, for production of multilayer ceramic devices by direct ink-jet overprinting of digital patterns. An ink of 14 vol% ceramic loading was used and a pattern of accumulated height of ~1.5 mm was printed [21]. In the present work, a printing table fitted with an advanced multi-nozzle monocolour Xaar ink-jet print head XJ500 and with 'z' direction control was used for making pillar arrays. A loading of 14 vol% ZrO₂ and a high ceramic volume fraction (0.63) based on the dried ink were formulated and processed. The issues that influence the printing of pillars are registration, the extent of forced ink drying and the ceramic volume fraction based on the dried ink.

2. Experimental details

2.1. Ink preparation

The ZrO₂ powder was HSY3 (ex Daiichi-Kigenso, Japan) having a quoted average particle size of 0.45 μm and a surface area of 7 m²/g. The dispersant was Solsperse 13940 (ex Zeneca Pigments and Additives, Manchester, UK) supplied in 40 wt% solution in an aliphatic solvent. A TEM micrograph of the powder shown in Fig. 1, indicates that the particles are equiaxed and confirms that the quoted particle size is a result of agglomeration. The ink was formulated to give a ZrO₂ powder volume fraction of 0.65 based on the dried ink and 14.2 vol% based on the solvated ink. The exact value after mixing was found by loss on ignition. The ink composition is given in Table I.

The procedure for making the ink was as follows. First a 20 vol% isopropyl alcohol (IPA)-octane solution was made, into which the dispersant and half the wax was added. This mixture was stirred until the wax dissolved. Zirconia powder was then added. The resulting mixture was stirred with an ultrasonic probe

*Present Address: Department of Materials, University of Cambridge, Pembroke Street, Cambridge CB2 3QZ, UK.

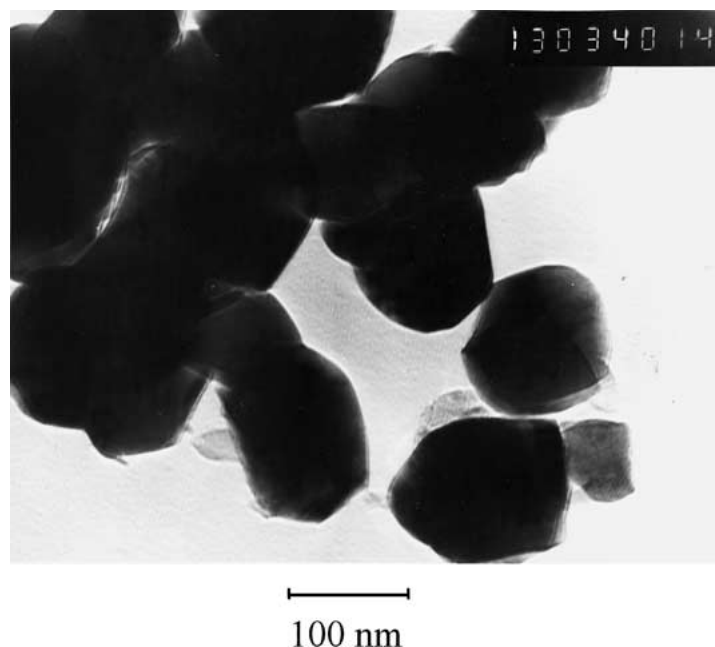


Figure 1 Transmission electron micrograph of the zirconia powder.

TABLE I Ink composition

Material	ZrO ₂ powder	Solsperse 13940	IPA ^a	Octane	Wax
vol%	14.21	11.85	14.21	56.89	2.84

^aIPA: isopropyl alcohol.

TABLE II Bead mill operating conditions

Variable	Tip speed	Flow rate	Temperature	Current
Value	14 m/s	1.42 ml/s	40°C	2 A

for 5 minutes and then milled in a high energy bead mill (KDL Dyno Mill ex Glen Creston, Stanmore, UK), charged with 0.5 mm diameter zirconia beads, to break down the agglomerates and disperse the powder in liquid. The operating details are shown in Table II. Care was taken to ensure that the temperature did not exceed 40°C and a braided wire was used to earth the fittings on the nylon end cap to prevent electrical discharge caused by tribo-electric effects in the mill when run with non-conducting inflammable liquids. The ink was passed through the mill six times with a total milling time of about 30 minutes. Finally the remaining half of the wax was added to the ink and the container was rotated overnight. After filtration through a 5 μm mesh, the ink was ready for use.

2.2. Printer operation

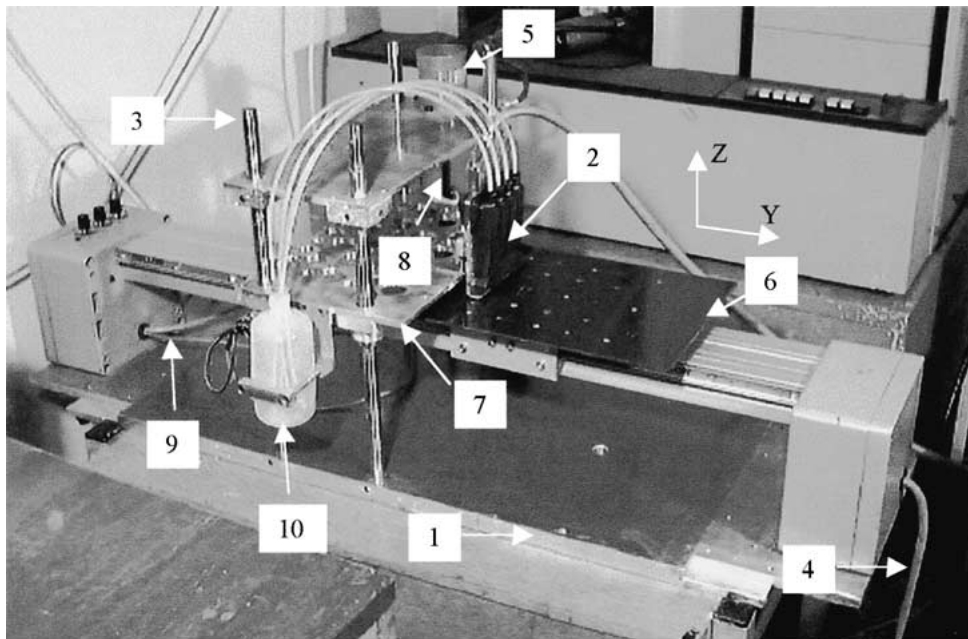
The printer consisted of a printing table (Fig. 2) that prints with a piezoelectric XJ500 monocolour print head. A MC202 controller for the sliding table and print head movement and a XaarJet PCI interface adapter for print head operation were fitted. The block control diagram is shown in Fig. 3. The control program was written in C++ and operated from the Visual C++ workspace.

The XJ500 print head is a 500 nozzle, in-line, piezoelectric drop-on-demand array with a print width of 70 mm and nozzle diameters of 50 μm, capable of print-

ing two dimensional images of maximum width 70 mm. No X-direction translation is therefore needed. The data for the image files, in device independent bitmap (DIB) format, were sent to the print head by means of a stroke engine, a shaft encoder and a product detector, which co-ordinates and controls the firing of the ink from the nozzle and the movement of the sliding table for each pass of printing. The sliding table moved to the end of the track behind the print head after each pass of printing where it re-registered its initial position ready for the next pass. A hot air-blower was mounted at the end of the track to dry the printed image. The gap between the nozzle plate and the printing surface was maintained at about 1 mm by the control program typically for every 0.1 mm of accumulated image thickness.

The ink reservoir was attached to the side of the print-head mounting plate (Fig. 2) so that the ink level could be adjusted. During printing, the recommended ink level is 10–40 mm below the nozzle plate and it was kept at ~30 mm below the nozzle plate for the work carried out here. An airtight cap to the nozzle plate was used for filling the print head to prepare for printing. The cap is connected to a syringe and during filling, the ink was aspirated from the bottle through the print head to the syringe and pushed back to the bottle several times until no bubbles were observed in the tubing.

Due to the nozzle arrangement and firing sequence, the sliding table was set to travel at about 500 mm/s when printing. The resulting resolution was 180 × 180 dpi. The substrate was silicone release paper (grade Steralease SL31, ex Sterling coated Materials, Hyde, Cheshire). After printing, the components were easily lifted from this substrate and pyrolysis was carried out in flowing air to remove the organic vehicle. A conservative heating schedule was used, namely: 60°C/hr to 60°C; 24 hr dwell; 5°C/hr to 400°C; 1hr dwell followed by furnace cooling. The zirconia was fired at 1450°C for 2 hours in air with a heating rate of 10°C/min.



- | | | | |
|---|---------------------------|----|-----------------------|
| 1 | chassis | 2 | print head |
| 3 | guiding pillar | 4 | cable to Y-step motor |
| 5 | Z-step motor | 6 | sliding table |
| 7 | mounting plate | 8 | lead screw |
| 9 | cable to position sensors | 10 | ink bottle |

Printing table for ceramic overprinting

Figure 2 The arrangement of the Xaar print-head on a z-displacement gantry over the moving table.

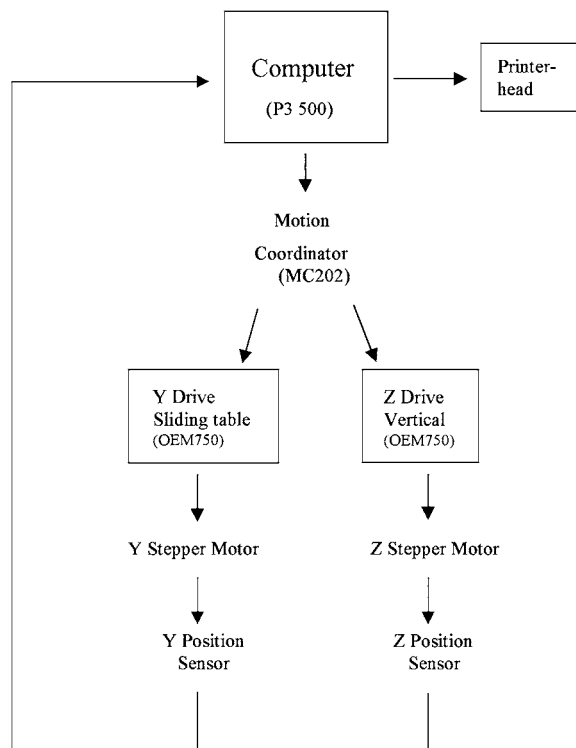


Figure 3 Schematic diagram of the printer control sequence.

3. Results and discussion

Arrays of 11×16 pillars were printed onto $8 \text{ mm} \times 12 \text{ mm}$ rectangular bases consisting of 400 layers of the same ink. The spacing between adjacent pillars was

5 dots corresponding to $710 \mu\text{m}$ in both X and Y directions. Some arrays of 11×12 pillars were also printed on bases of the same size to give a spacing between pillars in the Y direction of 7 dots ($847 \mu\text{m}$). This was due to concerns over the mechanical accuracy in the Y direction, which proved to be overcautious. In fact pillar arrays of finer spacing can be produced and the spacing is limited by droplet flow and coalescence, in turn controlled mainly by drying behaviour.

The block of 400 passes was printed first to give, based on previous experience [21], an as-printed thickness of $\sim 0.7 \text{ mm}$. After depositing each layer, the printed pattern was dried at the end of the table for 20 seconds by the hot air-blower. The temperature at the sample surface was about 45°C measured with a fine thermocouple. A longer time slowed down the printing process. A shorter time was not sufficient for adequate drying and led to ink spreading and imperfect growth of pillars. Each pass took approximately 30 s.

Within the print head there is about 20 ml of ink. Generally it took more than 6 hours to consume 20 ml of ink, so that some ink stayed in the print head for this length of time. Although the sedimentation of the ink was not directly observable, the ink near the nozzle plate (at the bottom of the print head) tended to become much thicker after several hours of printing. The symptom this presented was that less ink was emitted in each ejected ink drop because of the higher viscosity of the ink. The printed image, captured intermittently on transparent acetate test strips inserted manually under

the print-head, became progressively fainter until the printing process ceased altogether. To prevent this, the print-head was flushed (or re-filled) with fresh ink every 100 passes to ensure the quality of the printed image. The practical consequence of this is possible sedimentation in the nozzle and therefore in mass production the nozzle should be modified to accommodate constant recirculation of ink across the entry to the ink chambers.

Despite flushing the nozzles, the image at the end of each 100 passes was fainter than that at the end of 100 passes when printing the solid base. This is because the print density is considerably less when printing pillars, much less ink was consumed on each pass and the residence time in the nozzle was higher. This permits more sedimentation and although the nozzle did not block, the ink near the nozzle plate became more viscous. This thickening effect has implications for integrity of rendering of the design and for quality control.

For the first 3500 passes, the print head was flushed every 100 passes. The total height of the pillars after 3500 passes was about 1mm, which made each layer $\sim 0.3 \mu\text{m}$. This value is far less than the height of $\sim 1.8 \mu\text{m}$ for each layer of the printing of solid blocks [21]. This is mainly due to the fact that the registration in the 'y' direction was not sound. Instead of repeatedly depositing an ink drop on the same spot, the ink drop was deposited in different spots along a short line on each pass, so that the intended pillars actually became blades with an aspect ratio of about 3 : 1. Obviously when printing a solid slab, slight mis-registration is only noted at the edges and the overall build height is unaffected. After 3500 passes, the printer head was flushed every 50 passes until the printing finished at 4900 passes. The final height at 4900 passes was approximately 2 mm, which makes the layer height about $0.7 \mu\text{m}$ for the last 1400 passes.

Fig. 4 shows the general area of the building site with blocks of pillar arrays at various stages of construction. Some have been removed for characterisation. They

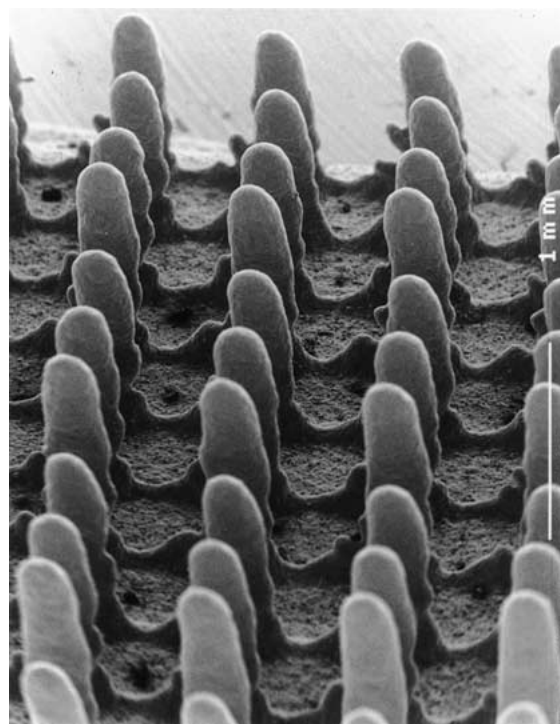


Figure 5 Scanning electron micrograph of partly built and then sintered arrays (3500 passes) showing signs of mis-registration in the direction of table travel.

are easily removed from the release paper with a thin palette knife.

Fig. 5 shows a scanning electron micrograph of the pillar array printed to 3500 layers giving an average pillar height of about 1.3 mm. In this example, the array was removed from the building site during construction, the organic components of the ink were removed by pyrolysis and the assembly sintered at 1450°C . It can immediately be seen that in the direction of table traverse the registration problem has caused elongation of the pillars into blades and produced a continuous sub-wall

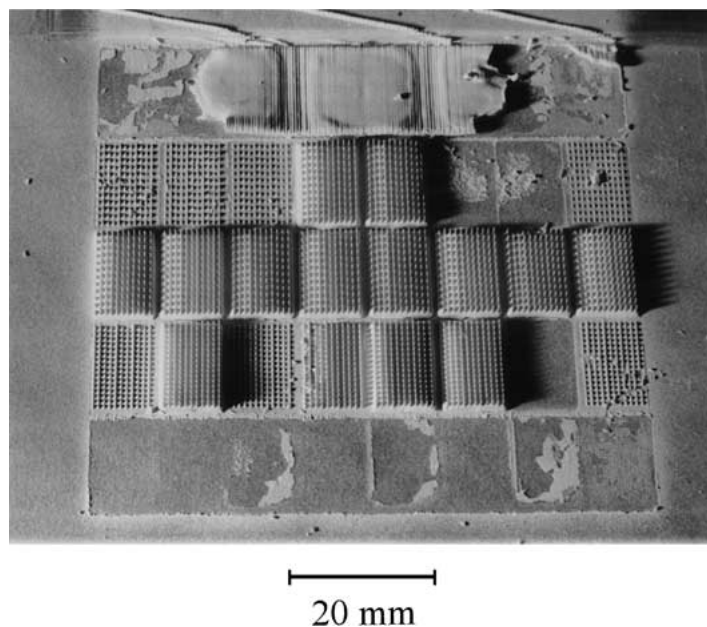


Figure 4 Photograph of the building site showing blocks of pillar arrays; some have been removed for testing.

connecting rows. This was caused by the method of re-setting the table travel at the end of each traverse and was a problem that could be ameliorated to some extent by modifications to the control program.

Loss on ignition showed that the dried ink contained 91.7 wt% ZrO_2 compared with the intended 92.5 wt% based on the formulation (Table I). This corresponds to a volume fraction of 0.63 based on the dried ink taking account of loss of all solvent (that added and the 60% solvent present in the dispersant). The linear shrinkage between printing and sintering was $19.3 \pm 0.7\%$ (the error is the 95% confidence interval) whereas the calculated linear shrinkage based on particle packing is 13%. The additional shrinkage is partly due to resid-

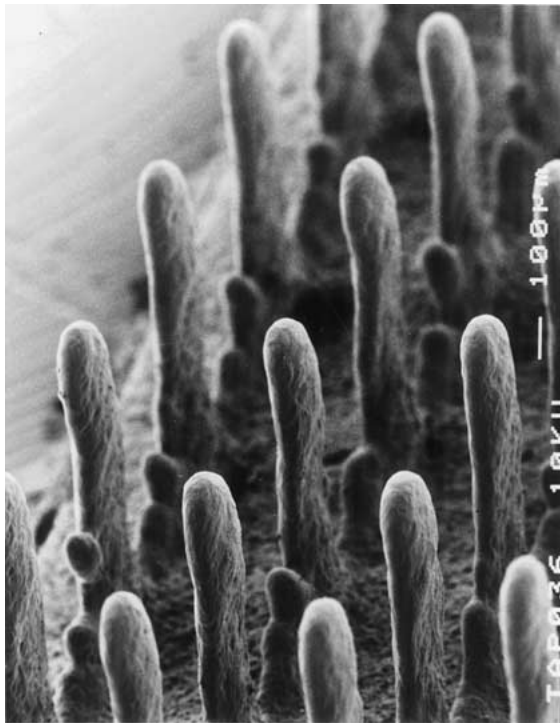


Figure 6 Sintered arrays of pillars built to 4900 passes; slight mis-registration problems remain but there are no signs of slumping during the pyrolysis stage.

ual solvent from the dispersant, which is less volatile than the octane and partly to imperfect packing during droplet drying accelerated by the warm air blower.

Fig. 6 shows the pillars printed to 4900 layers and sintered. The average pillar height is about 2 mm before sintering. Near the base of each pillar, it can be seen that the registration problem described above has not been entirely solved and small nodules have grown near the base of the pillars as a result of systematically misplaced droplets. The pillars suffered little or no deformation indicating that ceramic/binder ratio of 0.63 was high enough to prevent slumping during binder removal.

Fig. 7 shows typical surface microstructure of the ceramic pillars after sintering. The outer surface shows the ripples associated with each droplet relic. Similar freeforming relics are noted in the surface of models built by stereolithography, selective laser sintering and fused deposition modelling. The elongation of the pillar is clearly seen to result from the offset of droplets.

In previous work [21] it was shown that the fracture surfaces of sintered ceramics made by ink-jet printing were smooth and featureless and hence free from droplet relics. Fig. 8 shows the fracture surface of a pillar similar to those shown in Fig. 6. Although the surface is relatively smooth, it is possible to detect concentric features that at first sight appear to be associated with droplet relics namely the intersection of the fracture path with dome-shaped contours at droplet boundaries. The more likely explanation is connected with drying shrinkage. The pillars are high surface area to volume ratio parts of the body that are close to elliptical in shape. A significant difference between this artefact and previous printed ceramics is that forced hot air circulation was needed to restrict ink flow and hence generate pillars. This rapid drying may have deleterious effects on microstructure if residual solvent remains at the centre of the pillars once the surface regions have dried. A similar effect was found to cause concentric cracks in helical ceramic windings [22] and this shows that the control of drying in direct ceramic ink-jet printing deserves more attention.

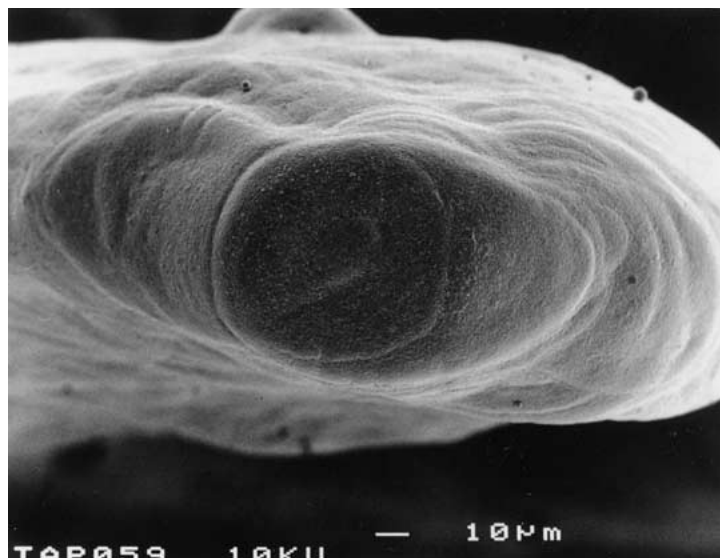


Figure 7 View from directly above a sintered pillar showing the surface pattern of droplet relics.

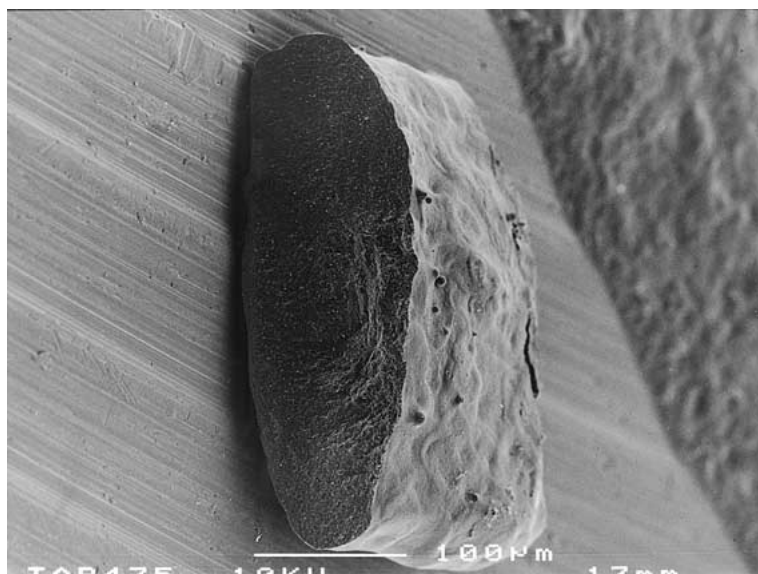


Figure 8 Fracture surface of a pillar; no internal droplet relics can be seen.

4. Conclusions

This work indicates that an ink based on a low electrical conductivity solvent with a ceramic loading of 14 vol% ZrO_2 can be subjected to direct ceramic ink-jet printing in a modern high performance wide array print-head. Using an improved ink design with 0.63 volume fraction ceramic in the dried ink and with 'z' direction control on the printer, ceramic pillars with sufficient height (~ 2 mm) can be created and subsequently sintered without deformation.

Acknowledgements

The authors are grateful for EPSRC for funding this work under grant No. GR/M07755 and to Angus Condie of Xaar for the loan of a Xaar printing system.

References

1. P. F. BLAZDELL, J. R. G. EVANS, M. J. EDIRISINGHE, P. SHAW and M. J. BINSTED, *J. Mater. Sci. Lett.* **14** (1995) 1562.
2. Q. F. XIANG, J. R. G. EVANS, M. J. EDIRISINGHE and P. F. BLAZDELL, *J. Eng. Manuf.* **211B** (1997) 211.
3. J. H. SONG, M. J. EDIRISINGHE and J. R. G. EVANS, *J. Amer. Ceram. Soc.* **82** (1999) 3374.
4. B. Y. TAY and M. J. EDIRISINGHE, *J. Mater. Res.* **16** (2001) 373.
5. P. F. BLAZDELL and J. R. G. EVANS, *J. Mater. Proc. Tech.* **99** (2000) 94.
6. C. E. SLADE and J. R. G. EVANS, *J. Mater. Sci. Lett.* **17** (1998) 1669.
7. M. J. WRIGHT and J. R. G. EVANS, *ibid.* **18** (1999) 99.
8. K. A. M. SEERDEN, N. REIS, B. DERBY, P. S. GRANT, J. W. HALLORAN and J. R. G. EVANS, *Proc. MRS Symp.* **542** (1999) 141.
9. M. MOTT, J. H. SONG and J. R. G. EVANS, *J. Amer. Ceram. Soc.* **82** (1999) 1653.
10. M. MOTT and J. R. G. EVANS, *Mat. Sci. Eng. A.* **271** (1999) 344.
11. A. ATKINSON, J. DOORBAR, A. HUDD, D. L. SEGAL and P. J. WHITE, *J. Sol-Gel. Sci. and Tech.* **8** (1997) 1093.
12. M. MOTT and J. R. G. EVANS, *J. Amer. Ceram. Soc.* **84** (2001) 307.
13. M. L. GRIFFITH and J. W. HALLORAN, *ibid.* **79** (1996) 2601.
14. D. L. BOURELL, H. L. MARCUS, J. W. BARLOW and J. J. BEAMAN, *Int. J. Powder Metal.* **28** (1992) 369.
15. R. SOUNDARARAJAN, G. KUHN, R. ATISIVAN, S. BOSE and A. BANDYOPADHYAY, *J. Amer. Ceram. Soc.* **84** (2001) 509.
16. R. E. NEWNHAM, D. P. SKINNER and L. E. CROSS, *Mat. Res. Bull.* **13** (1978) 525.
17. A. SAFARI, V. F. JANAS and A. BANDYOPADHYAY, *A. I. Ch. E. Journal* **43** (1997) 2849.
18. H. TAUNAUMANGH, I. L. GUY and H. L. W. CHAN, *J. Appl. Phys.* **76** (1994) 484.
19. M. DALBY, L. DI SILVIO, G. DAVIES and W. BONFIELD, *J. Mat. Sci: Mat. In Medicine* **12** (2000) 805.
20. A. R. BHATTI, M. MOTT, J. R. G. EVANS and M. J. EDIRISINGHE, *J. Mat. Sci. Lett.*, in press.
21. G. THORNELL, L. KLINTBERG, T. LAURELL, J. NILSSON and S. JOHANSSON, *J. Micromech. Microeng* **9** (1999) 434.
22. X. ZHAO, J. R. G. EVANS, M. J. EDIRISINGHE and J. H. SONG, to be published.
23. J. K. WRIGHT, R. M. THOMSON and J. R. G. EVANS, *J. Mater. Sci.* **25** (1990) 149.

Received 20 July 2001
and accepted 30 January 2002